



Received on 26 February, 2018; received in revised form, 04 May, 2018; accepted, 13 May, 2018; published 01 October, 2018

SYNTHESIS OF SILVER NANOPARTICLES USING SWERTIPUNICOSIDE AND ITS ACTIVITY ON HUMAN BREAST CANCER CELL LINE (MCF-7)

S. Sivaranjani and C. Arulvasu *

Department of Zoology, University of Madras, Guindy Campus, Chennai - 600025, Tamil Nadu, India.

Keywords:

Swertipunicoside,
Electron microscope,
Silver nanoparticles, XRD

Correspondence to Author:

Dr. C. Arulvasu

Assistant Professor,
Department of Zoology,
University of Madras, Guindy
Campus, Chennai - 600025,
Tamil Nadu, India.

E-mail: carulvasu@gmail.com

ABSTRACT: In the current study, synthesis of silver nanoparticles (AgNPs) using swertipunicoside was tested against human breast cancer cell line (MCF-7). The swertipunicoside was tested against the normal cell line such as vero cells to find out the toxicity of the compound. The synthesized AgNPs were characterized using UV-visible spectroscopy, x - ray powder diffraction (XRD), fourier-transform infrared spectroscopy (FTIR) and field-emission Scanning Electron Microscope (FESEM) with energy dispersive spectroscopy (EDAX). The synthesized silver nanoparticles was checked with the colour variation and it was confirmed by UV-vis spectral analysis. The morphology of the synthesized nanoparticles were analysed using FESEM along with EDAX. The XRD was done to find out the crystalline structure of the compound. FTIR measurements are carried out to identify the possible biomolecules responsible for capping and efficient stabilization of the silver NPs synthesized using swertipunicoside. The synthesized AgNPs and swertipunicoside was tested against the MCF-7 cell line to find out the cell viability. Our results showed that the compound and synthesized silver nanoparticles inhibited the proliferation of human breast cancer cell line with an IC_{50} value of 60 mg/ml and IC_{50} of 40 μ g/ml at 24 h incubation. From this study, concluded that swertipunicoside and synthesized AgNPs have potential anticancer activity.

INTRODUCTION: Breast cancer is the second most common cause of cancer death in women ^{1, 2}. Many cancers initially respond to chemotherapy, and later they develop resistance ^{3, 4, 5}. Breast cancer originates from the breast tissue, especially from the inner lining of milk ducts or lobules. It results from a multistep process, which involves initiation, promotion and progression ⁶. The development of breast cancer involves several proteins and genes, namely; CDK 2 (Cyclin dependent kinase), VEGF (Vascular endothelial growth factor), HIF 1 (Hypoxia-inducible factors), AP 1 (Activator protein), p53, p57, cyclin A and B ⁷.

Environmental and internal factors; for example smoking and oestrogen have been claimed to be the risk factors for breast cancer ⁸. Due to drug resistance and poor prognosis, low success rates have been observed in the management of breast cancer that necessitated the use of complementary and alternative medicine (CAM) and natural health products like dietary polyphenols ⁹.

Currently available chemopreventives and chemotherapeutic agents cause undesirable side effects ^{10, 11}, therefore developing a biocompatible and cost effective method of treatment for cancer is indispensable. The development of nanotechnology has been a boon to mankind as its significance paved the way for several applications in therapeutics ¹², catalysis ¹³, microelectronics, biosensing devices ¹⁴, air and water purifiers, paints ¹⁵, and so forth. Recently, silver nanoparticles have gained much interest among the emerging nano-

QUICK RESPONSE CODE 	DOI: 10.13040/IJPSR.0975-8232.9(10).4393-01
	Article can be accessed online on: www.ijpsr.com
DOI link: http://dx.doi.org/10.13040/IJPSR.0975-8232.9(10).4393-01	

products in the field of nanomedicine due to their unique properties and obvious therapeutic potential in treating a variety of diseases. The nanoparticles can be synthesized by physical, chemical, and biological methods. In the medical aspects, applications of nanoparticles increased tremendously only when the biological approach for nanoparticle synthesis came into focus. Currently, a variety of cytotoxic agents have been used in the treatment of breast cancer, such as doxorubicin, cisplatin, and bleomycin^{16, 17}. Although usage of doxorubicin, cisplatin, and bleomycin provides beneficial effect, but the efficacy and demerits are uncertain¹⁶.

Swertia punicea tastes extremely bitter, possesses the ability to reduce fever and detoxify, and is used in the South-Western part of China for the treatment of hepatogenous jaundice and cholecystitis. No chemical studies have previously been reported for *S. punicea*. Investigation of the whole plant of *S. punicea* has led to the isolation, from the n-BuOH fraction of the EtOH extract, of the first member of a new series of natural products, a bisxanthone C-glucoside, swertipunicoside¹⁸. So, it is necessary to find novel therapeutic agents against cancer, which are biocompatible and cost effective. Therefore, this study was designed to synthesize AgNPs using swertipunicoside and to evaluate potential toxicity and the general mechanism of synthesized AgNPs in human breast cancer cells (MCF-7 cells).

MATERIALS AND METHODS:

Synthesis of Silver Nanoparticles: Swertipunicoside was gifted from Niscell stem cell lab, Malaysia. Silver nitrate GR was purchased (Merck, India) 100 mL. Aqueous solution of silver nitrate (AgNO_3) (sigma-aldrich) were prepared with 1 mM solution of silver nitrate was prepared with double distilled water. A known volume of 1, 2, 3, 4 and 5 mL of swertipunicoside was added separately to aqueous solution. The effect of dark room temperature on the synthesis of silver nanoparticles was carried out¹⁹.

Characterization of Silver Nanoparticles: UV-vis spectroscopic analysis of silver colloidal dispersion showed peak at 420 nm confirming the synthesis of AgNPs. The reason for formation of AgNPs was attributed to the presence of flavonoids and polyphenols in swertipunicoside.

The structure and size of synthesized silver nanoparticles were analysed using the FESEM along with EDAX operating at an accelerating voltage of 15.0 kV with a point resolution and Cs of 9.8 mm and 12.0k SE. To confirm the purity of silver nanoparticles, an EDAX (FEI, USA) spectrum of silver colloidal dispersion was recorded by initially spotting the sample in electron microscope followed by estimation of its elemental composition. EDAX spectrum displays clear identification peaks of major energies of silver confirming the presence of silver in AgNPs. Signal of aluminium is due to the background from supporting aluminium grid used as the sample cell.

This validates that the phytochemicals of swertipunicoside play a key role in capping and stabilization of AgNPs²⁰. Fourier transform infrared (FTIR) spectral measurements were carried out to identify the potential biomolecules in swertipunicoside which is responsible for reducing and capping the bioreduced silver nanoparticles. FTIR was performed on Thermo scientific™ Nicolet iS™50 FTIR spectrometer to detect the possible functional groups in biomolecules present in the compound. The X-ray diffraction (XRD) measurement was performed on X-ray diffractometer (Panalytical Xpert-PRO 3050/60) operated at 30 kV and 100 mA and spectrum was recorded by $\text{CuK}\alpha$ radiation with wavelength of 1.5406 Å in the 2θ range of 20° - 80°.

Cell Culture: Human breast cancer cells (MCF-7) was obtained from NCCS, Pune. The cells were maintained in Dulbecco's modified Eagle's medium (DMEM) supplemented with 10% fetal bovine serum (FBS) and 1% antibiotic-antimycotic solution was purchased from Hi-media. Cells were grown to confluence at 37°C with 5% CO_2 atmosphere. All experiments were performed in 96-well plates. Cells were seeded onto the plates at a density of 1×10^6 cells per well and incubated for 24 h prior to the experiments. 1 mg of compound and 1 mg of synthesized silver nanoparticles were first dissolved in 10 ml of double distilled water experiment was performed using varying concentrations of swertipunicoside (20, 40, 60, 80 and 100 mg/mL) and compared with synthesized AgNPs (20, 40, 60, 80 and 100 µg/ml) in varying concentrations and control.

At the end of 24 h the medium in each well was discarded and 10 μL of MTT (3-(4, 5-dimethylthiazol-2-yl)-2, 5-diphenyltetrazolium bromide) solution (5 mg/mL in phosphate buffer saline) was added to each well and the plate was incubated at 37 $^{\circ}\text{C}$. On completion of 4 h, DMSO (100 μL) was added to each well to dissolve formed formazan crystals and absorbance was recorded at 597 nm filter using ELISA plate reader (Lisa plus, India) to calculate percent cell viability.

Percentage of viability =

$$\frac{\text{OD value of experimental sample}}{\text{OD value of experimental controls}}$$

The cytotoxicity assay was followed by the method of ²¹. The cells were seeded at 1×10^5 cells / well

into a six well chamber plate and incubated overnight. Later, the medium was replaced with maintenance medium DMEM without FBS containing 60 and 40 mg/ml swertipunicoside at 24h in vero cell line. The cytomorphology was examined under Nikon inverted microscope. This endorses that phytochemicals present in swertipunicoside not only effectively reduced silver nitrate to AgNPs but also provide non-toxic surface coating for its biomedical applications.

RESULTS:

Characterization of Synthesized Silver Nanoparticles: Initially the swertipunicoside was yellow and upon providing the silver salt it turned from light brown colour to dark brown colour **Fig. 1**.

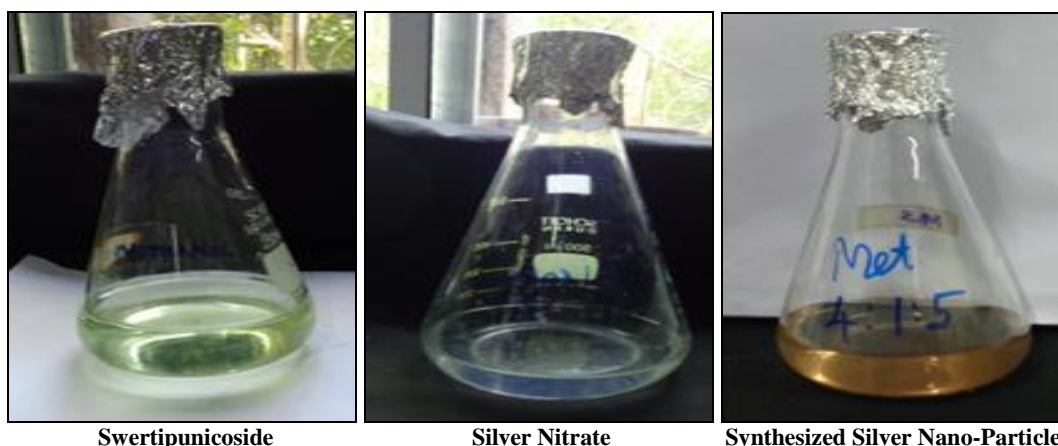


FIG. 1: COLOUR INTENSITY OF SYNTHESIZED AgNPs AT VARIOUS TIME INTERVALS

UV-Vis Spectral Analysis: The increased absorbance was observed at various time intervals (1 h difference upto 9 h) and the peak at 420 nm correspond to the surface plasmon resonance of silver nanoparticles. It is reported earlier that absorbance at around 430 nm for silver is a characteristic of these noble metal particles. The absorption spectra of silver nanoparticles with different diameters.

The maximum absorption peaks (λ_{max}) are located at 420, 422, 424, 428 and 430 nm, respectively. The absorption peaks shift red with the increase of diameters of silver nanoparticles showed in **Fig. 2**. The presence of nanoparticles was confirmed by obtaining a spectrum in UV-Vis range from 200 - 800 nm. The peak at 430 nm confirmed the synthesis of silver nanoparticles ²².

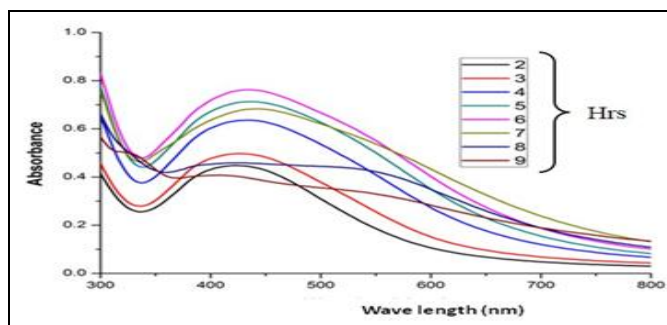


FIG. 2: UV SPECTRAL PEAK OF AgNPs SYNTHESIZED AT DIFFERENT HOURS

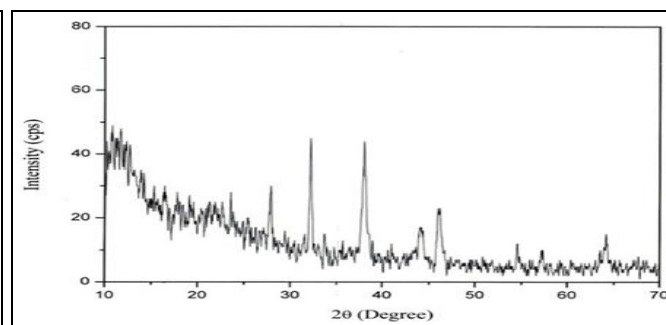


FIG. 3: XRD PATTERN OF AgNPs EXHIBITING THE FACETS OF CRYSTALLINE SILVER

XRD Analysis: The XRD patterns of vacuum to confirm the crystalline nature of the particles, and the XRD pattern showed the number of Bragg's reflections that may be indexed on the basis of the face centered cubic structure of silver. In order to verify the results of UV-Vis spectral analysis, the sample of silver ions exposed to swertipunicoside were examined by XRD. The silver nanoparticles synthesized were calculated by the particle size ranges of the silver at 32 nm and 38 nm corresponding to swertipunicoside shows the XRD spectrum corresponding to Ag. The strongest peak is observed at 32° which corresponds to the predominant growth in the direction of (1 1 1) plane. The two characterization peaks for Ag metallic system reveal that they are crystallized in FCC structure. All reflections in the XRD pattern resemble to that of monometallic counterparts showed in **Fig. 3**.

FTIR Analysis: FTIR band intensities in different regions at the spectrum for the synthesized silver nanoparticles. The IR absorption bands at 3439 cm^{-1} , 1062 cm^{-1} and 782 cm^{-1} in the spectrum correspond to the OH stretching vibration of phenolic hydroxyls stretching vibrations of NH^{2+} and NH^{3+} in protein/peptide bonds, carbonyl stretching in proteins and COH vibrations and proteins present in swertipunicoside. The relative decrease in the intensity of phenolic hydroxyl stretching band in the spectrum of swertipunicoside functionalized BMNPs indicate the partial role of phenolic hydroxyls in the reduction mechanism by donating electrons and forming quinones. The appearance of band at 3439 cm^{-1} in the functionalized spectrum of Ag correspond to the CO stretching modes derived from swertipunicoside. The dual role of the swertipunicoside as a reducing

and capping agent and presence of some functional groups was confirmed by FTIR analysis of silver nanoparticle. A broad band between 3439 cm^{-1} is due to the N-H stretching vibration of group NH_2 and OH the overlapping of the stretching vibration of attributed for water and swertipunicoside molecules.

The band at 1636 cm^{-1} corresponds to amide $\text{C}=\text{O}$ stretching and a peak at 2953 cm^{-1} can be assigned to alkyne group present in swertipunicoside. The observed peaks at 1183 cm^{-1} denote $-\text{C}-\text{O}-$ linkages, or $-\text{C}-\text{O}-$ bonds showed in **Fig. 4**. From FT-IR results, it can be concluded that some of the compounds from swertipunicoside formed a strong coating/capping on the nanoparticles.

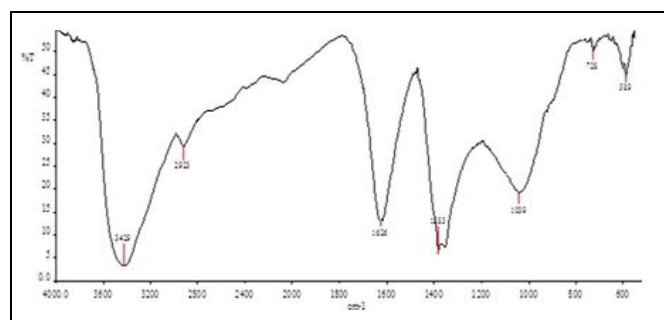


FIG. 4: FTIR BAND PEAKS SHOWING THE OXIDIZED BIOMOLECULES IN AgNPs SYNTHESIS

FESEM Analysis: The FESEM micrograph shows the synthesized AgNPs were uniformly aggregated **Fig. 5**. The EDAX attachment with the FESEM was known to provide information on the chemical analysis of the fields that are being investigated to specific locations. This represents well dispersed AgNPs, and the size range of 50 to 400 nm was observed in the FESEM images of the synthesized AgNPs. The presence of elemental silver can be observed in the graph obtained from EDX analysis.

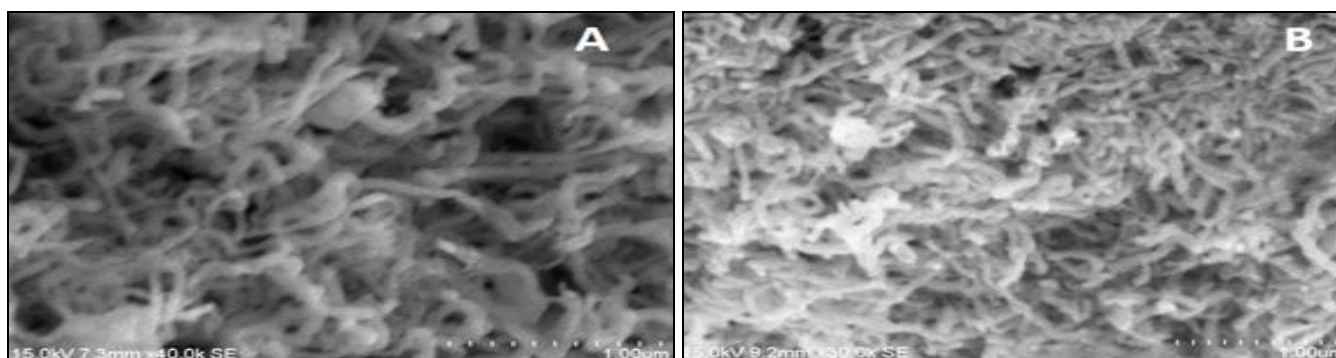


FIG. 5: TOPOGRAPHICAL RESULTS OF SWERTIPUNICOSIDE (A) AND AgNPs (B) CONFIRMING THE UNIFORM AND AGGREGATES FORMED DURING FESEM ANALYSIS

In EDAX spectrum, the peak positions at 0.261, 0.250, 0.245, 2.629 keV represents the binding energies of the swertipunicoside and representing

the dispersed nanoparticles of irregular shape with average size of 50 - 200 nm showed in **Fig. 6**.

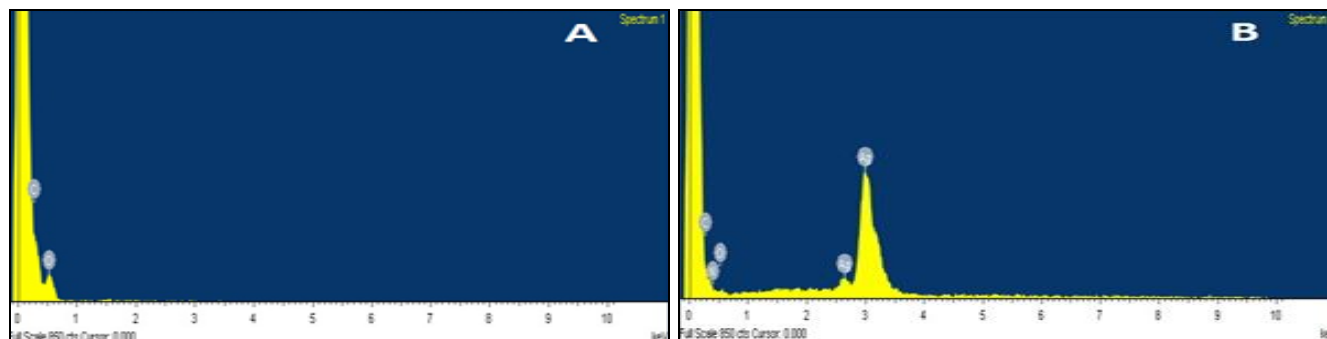
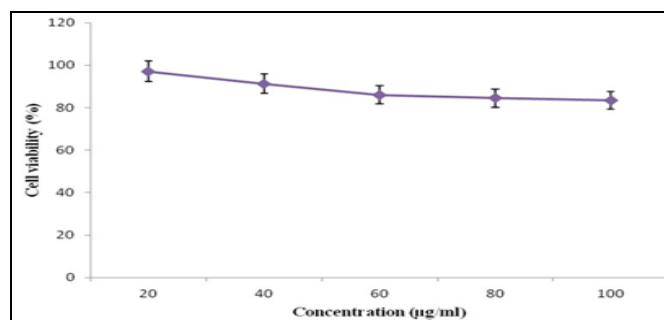


FIG. 6: ENERGY DISPERSIVE X-RAY SPECTRUM OF SWERTIPUNICOSIDE (A) AND SILVER NANOPARTICLES (B)

Cytotoxicity: Microscopic observations were monitored using Nikon light inverted microscope wherein treated cells showed distinct cellular morphological changes indicating unhealthy cells, whereas the control appeared normal cell line. The normal cell line such as African monkey kidney cell line (vero cell line) was treated with various concentration of swertipunicoside to find out the toxicity showed in the **Graph 1**. The result shows 90% of cell survival. The synthesized silver nanoparticles were found to be non toxic at 500 mg/ml concentration. Control cells were irregular confluent aggregates with rounded and polygonal cells.

Morphological Observation: Swertipunicoside analogs Q-Cl and Q-OCH₃ also show some activity against the breast cancer cell line MCF-7

with 70% and 60% cell survival in 24 h, respectively. A major mechanism reported for the activity of swertipunicoside against estrogen dependent breast cancer is inhibition of Type II estrogen binding sites (ER II).



GRAPH 1: EFFECT OF DIFFERENT CONCENTRATION OF SWERTIPUNICOSIDE ON VERO CELLS AFTER 24 h INCUBATION

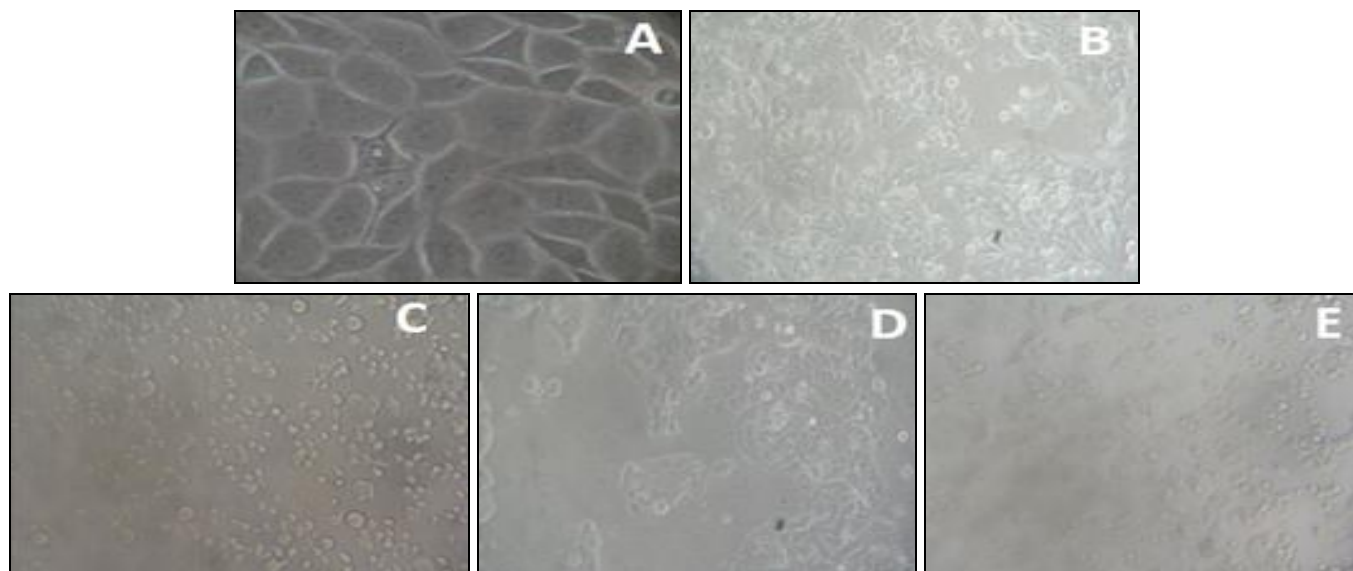


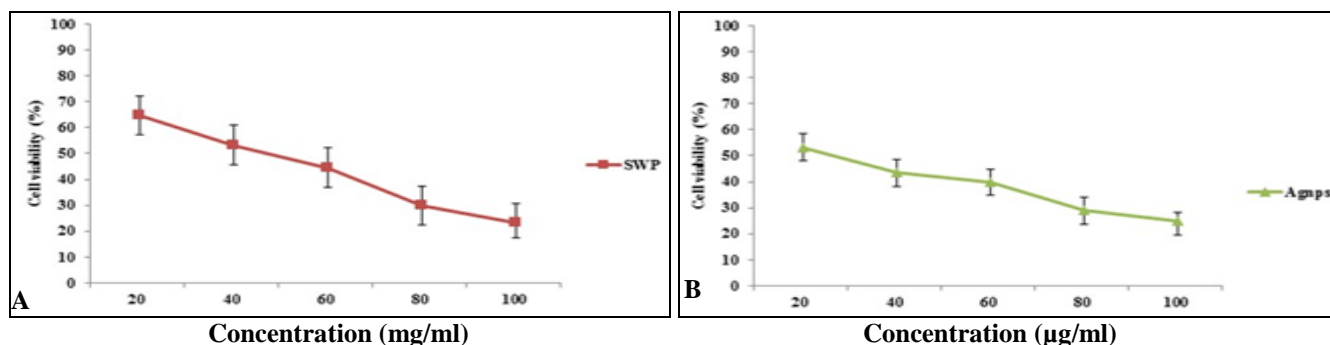
FIG. 7: MORPHOLOGICAL OBSERVATION OF CONTROL AND CELLS (MCF-7) TREATED WITH SWERTIPUNICOSIDE AND AgNPs AT 24 h (40 × MAGNIFICATION) (A) CONTROL (MCF-7); (B) IC₅₀ CONCENTRATION SWERTIPUNICOSIDE 60 mg/ml (C) MAXIMUM CONCENTRATION SWERTIPUNICOSIDE 100 mg/ml (D) IC₅₀ CONCENTRATION AgNPs 40 µg/ml (E) MAXIMUM CONCENTRATION AgNPs 100 µg/ml

Estradiol possesses the growth stimulatory effect in the estrogen-dependent breast cancer. Swertipunicoside is reported to bind to ER II. Although details of binding of swertipunicoside have not been reported. Absence of such hydroxyl groups is probably responsible for the reduced activity of two analogues Q-Cl and Q-OCH₃. The reduced activity of the analogues may play a role in the breast cancer. Exploring the structural modifications of swertipunicoside further so as to include a combination of one of the two hydroxyl groups among 5 and 7 and one from 3' or 4' position may be helpful in throwing light on this aspect. Control cells were irregular confluent aggregates with rounded and polygonal cells.

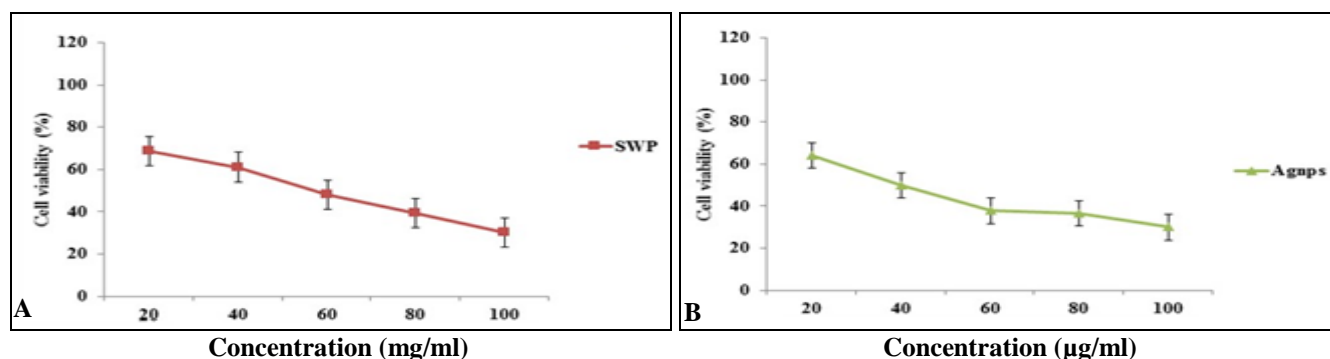
The IC₅₀ value of swertipunicoside was obtained at the concentration of 60 mg/ml and 100 mg/ml was used as a maximum concentration at 24 h. The swerti-punicoside treated cells are shrink, spherical and aggregated when compare to control. The IC₅₀ value of synthesized AgNps was obtained at the concentration of 40 µg/ml and 100 µg/ml was used as a maximum concentration at 24 h incubation. Synthesized AgNps treated cells appeared to shrink more, became spherical in shape, cell spreading patterns were restricted and cells are detached when compared to control **Fig. 7**.

Cell Viability: The MCF-7 cells were treated with swertipunicoside and synthesized AgNPs, the cells appeared to shrink became spherical in shape and cell spreading patterns were restricted when compared to control. The concentration of the compound was gradually increased from 20 to 100 mg/ml. For MCF-7 cells **Graph 2** viability decreased from 60 mg/mL swertipunicoside. The IC₅₀ value of the compound is 60 mg/ml. The toxic effect of swertipunicoside here was more pronounced, though obviously less than that of silver for all the concentrations. The incubation time for the both compound and AgNps is 24 and 48 h. After 24 h incubation, an obvious decrease in cell viability compared to control was registered for AgNPs at 40 µg/mL, respectively. From 20 µg/mL up to 100 µg/mL, the AgNPs demonstrated high degree of toxicity. It is worth noting that at both incubation times such as 24 and 48 h, cell viability was gradually decreased when the concentration was increased.

There was a change in the percentage of cell viability in control and AgNPs treated MCF-7 cells. Hence, the inhibitory concentration at 50% (IC₅₀) was observed at 40 µg/ml **Graph 3** of AgNPs for MCF-7 cells.



GRAPH 2: EFFECT OF DIFFERENT CONCENTRATION OF SWERTIPUNICOSIDE (A) AND SYNTHESIZED SILVER NANOPARTICLES (B) ON MCF-7 CELLS AFTER 24 h INCUBATION



GRAPH 3: EFFECT OF DIFFERENT CONCENTRATION OF SWERTIPUNICOSIDE (A) AND SYNTHESIZED SILVER NANOPARTICLES (B) ON MCF-7 CELLS AFTER 48 h INCUBATION

By contrast, the same concentration (IC_{50}) of AgNPs treated for Vero (normal) cell line at the inhibitory level 72.8%. The activity of AgNPs on vero cell line was constantly less at experimented dilutions as compared with cancer cell line. From this study, this may be connected with the swertipunicoside aggregation and sedimentation in the cell medium leading to the decrease in concentration of biologically active particles. From this cell viability assay, the silver nanoparticles have more capacity to kill MCF-7 cells when compare to swertipunicoside. There is no drastic change in swertipunicoside treated cells when the time is increased, whereas the synthesized AgNPs treated cells causes variation in cell viability when the time is increased at 40 and 20 $\mu\text{g/ml}$ **Graph 2 and 3**.

DISCUSSION: In the present study, the human breast cancer cell line (MCF-7) activity of swertipunicoside and cell viability variations of synthesized AgNPs were noted. The silver nanoparticle was synthesized using swertipunicoside. The colour was changed from yellow to brown colour. This clearly shows the synthesis of silver nanoparticles. The synthesis was confirmed by UV-vis spectrophotometer. It have been reported the silver nanoparticles starting from light yellow to dark brown. The absorption spectra of silver nanoparticles twisted in the reaction media have absorbance peak at 420 nm. The development of silver nanoparticles using swertipunicoside was viewed by the colour change²³. It has been reported that the XRD patterns of vacuum dried AgNPs synthesized using fluoresced peaks at 2θ values of 21.64° , 29.48° , 38.84° , 43.28° and 53.48° assigned to the (200), (101), (144), (202) and (311) planes of a face centered cubic lattice of silver.

Therefore XRD results also suggest that crystallization of the bioorganic phase occurs on the plane of the AgNPs³⁸. The FTIR analysis was carried out to find the presence of biomolecules present in the synthesized silver nanoparticles. The complete disappearance of the NH^{2+} and NH^{3+} stretching vibrations in the FTIR spectrum of BMNPs can be attributed to the breaking of amino acid residues of proteins during the reaction. Similar mechanism involving the role of phenolic hydroxyls and proteins in the reduction and stabilization of individual metal NPs have been

reported previously^{24, 25, 26, 27}. On the other hand, the extract sample prepared shows a wide and strong peak with maximum intensity at 529 cm^{-1} . The results are in good agreement with those found in literature²⁸. FESEM was used to find out the morphology of the compound and synthesized silver nanoparticles.

It is reported earlier that FESEM images for the biosynthesized silver nanoparticles cluster in shape with an average size ranging from 20 to 100 nm. The image confirms the formation of nanoparticles capped with its biomolecules. Metallic AgNPs generally show typical absorption peak approximately at 3 keV due to surface plasmon resonance²⁹. The elemental composition was revealed by energy dispersive X-ray spectroscopy (EDAS) attachment with the FESEM instrument³⁰. The swertipunicoside and synthesized silver nanoparticles was tested for cytotoxicity, cell viability and also morphological observation. The sensitivity of human cancer cell line for cytotoxic drugs is higher than that of vero cell line for the cytotoxic agents^{31, 32}. It probably takes place via optimally placed hydroxyl groups as in case of diethylstilbestrol³³. The HCT 15 cancer cell line showed distinct cellular morphological observation indicates the unhealthy cells whereas the control appeared normal. The control cells are irregular with rounded shape^{34, 35}. The cytotoxicity on HeLa cell lines were increased with increased concentration of AgNPs. There was a change in the percentage of cell viability in control and AgNPs (0, 5, 10, 20, 30, 40, and 50 $\mu\text{g/ml}$) treated HeLa cells^{36, 37}.

CONCLUSION: It is evident from the present study that the synthesis of silver nanoparticles is eco friendly, simple and efficient than the conventional method. The synthesis of silver nanoparticles was observed by colour variation and it was confirmed by UV-vis spectrophotometer. The characterisation of silver nanoparticle was done with FESEM along with EDAX, FTIR and XRD. The present studies suggest that the AgNPs are synthesized as well as stabilized by swertipunicoside. These synthesized nanoparticles highly inhibit the growth of cancer cells (MCF-7) have great importance as a therapeutic agent in preventing or lowering oxidative stress related to degenerative diseases, such as cancer.

ACKNOWLEDGEMENT: The authors are grateful to the UGC-UPE Phase - II, New Delhi for financial assistance.

CONFLICT OF INTEREST: There is no conflict of interest.

REFERENCES:

- Chan K and Morris GJ: Chemoprevention of breast cancer for women at high risk, *Seminars in Oncology* 2006; 33: 642-646.
- Jenal A, Thomas A and Murry T: Cancer statics, *CA: A Cancer Journal for Clinicians* 2002; 52: 23-37.
- Johnston SRD: Acquired tamoxifen resistance in human breast cancer - potential mechanisms and clinical implications, *Anti-Cancer Drugs* 1997; 8: 911-930.
- Kato S, Endoh, H and Masuhiro Y: Activation of the estrogen receptor through phosphorylation by mitogen-activated protein kinase, *Science* 1995; 270: 1491-1494.
- Lupu R, Cardillo M and Cho C: The significance of heregulin in breast cancer tumor progression and drug resistance, *Breast Cancer Research and Treatment* 1996; 38: 57-66.
- Kim MR, Choi HK, Cho KB, Kim HS and Kang KW: Involvement of Pin1 induction in epithelial- mesenchymal transition of tamoxifen resistant breast cancer cells. *Cancer Science*. 2009; 100 (10): 1834-1841.
- Sariego J: Breast cancer in the young patient. *Am. Surg* 2010; 12: 1397-400.
- Anuso E, Zuazo A, Irigoyen M, Urdaci MC, Rouzau A and Martínez-Irujo JJ: Flavonoids inhibit hypoxia-induced vascular endothelial growth factor expression by a HIF-1 independent mechanism. *Biochem. Pharmacol.* 2010; 79: 1600-1609.
- Jo KJ, Lee JM, Lee SC, and Park HR: Anticancer activity of persimmon (*Diospyros kaki* L.) calyx extracts on human cancer cells. *J Med Plants Res.* 2011; 12: 2546-2550.
- Brown K: Breast cancer chemoprevention: risk-benefit effects of the antioestrogen tamoxifen, *Expert Opinion on Drug Safety* 2002; 3: 253-267.
- Smith LL, Brown K and Carthew P: Chemoprevention of breast cancer by tamoxifen: risks and opportunities, *Critical Reviews in Toxicology* 2000; 30: 571-594.
- Liu H, Liu Y, Wang Z, He P: Facile synthesis of monodisperse, size-tunable SnS nanoparticles potentially for solar cell energy conversion, *Nanotechnology* 2010; 21(10): 0957-4484.
- Shin KS, Choi JY, Park CS, Jang HJ and Kim K: Facile synthesis and catalytic application of silver-deposited magnetic nanoparticles. *Catalysis Letters* 2009; 133: 1-7.
- Zhou L, He X, He D, Wang K and Qin D: Biosensing technologies for *Mycobacterium tuberculosis* detection: status and new developments, *Clinical and Developmental Immunology* 2011; 2011:1-8.
- Kumar PSS, Sivakumar R, Anandan S, Madhavan J, Maruthamuthu P and Kumar AM: Photocatalytic degradation of Acid Red 88 using Au-TiO₂ nanoparticles in aqueous solutions, *Water Research* 2008; 42: 4878-84.
- Franco - Molina MA, Mendoza - Gamboa E and Sierra-Rivera CA: Antitumor activity of colloidal silver on MCF-7 human breast cancer cells, *Journal of Experimental and Clinical Cancer Research* 2010; 29 (148): 1-7.
- Kim JS, Kuk E and Yu KN: Antimicrobial effects of silver nanoparticles, *Nanomedicine* 2007; 3: 95-101.
- Flora of China; Republica Popularis Sinicae, Science Press. 1988 (9): 344-349.
- Ahmed S, Saifullah, Ahmad, M, Swami BL and Ikram S: Green synthesis of silver nanoparticles using *Azadirachta indica* aqueous leaf extract. *Journal of radiation research and applied sciences* 2016 9(1); 1687-8507.
- Jadhav K, Dhamecha D, Bhattacharya D and Patil M: Green and eco-friendly synthesis of silver nanoparticles: Characterization, biocompatibility studies and gel formulation for treatment of infections in burns. *Journal of Photochemistry and Photobiology, B: Biology* 2016; 155: 109-115.
- Manikandan R, Beulaja M, Arulvasu C, Sellamuthu S, Dinesh D and Prabhu D: Synergistic anticancer activity of curcumin and catechin: an *in-vitro* study using human cancer cell lines. *Microsc Res Tech.* 2012; 75: 112-6.
- Sondi B and Salopek-Sondi J: *Colloid Interface Sci.* 2004; 275: 177.
- Babu G, Arulvasu C, Prabhu D, Jegadeesh R and Manikandan R: Biosynthesis and characterization of silver nanoparticles from *Datura innoxia* and its apoptotic effect on human breast cancer cell line MCF-7. *Materials letters* 2014; 98-102.
- Abid JP, Wark AW, Brevet PF and Girault HH: Preparation of silver nanoparticles in solution from a silver salt by laser irradiation. *Chemical Communications.* 2002; 792-793.
- Eutis S, Krylova G, Eremenko A, Smirnova N, Schill AW and El - Sayed M: Growth and fragmentation of silver nanoparticles in their synthesis with a FS laser and CW light by photo-sensitization with benzophenone. *Photochem Photobiol Sci.* 2005; 4: 154-159.
- Zhang, Yu JC, Yip HY, Li Q, Xu KW and Kwong AW: Ambient light reduction strategy to synthesize silver nanoparticles and silver-coated TiO₂ with enhanced photocatalytic and bactericidal activities. *Langmuir* 2003; 19: 10372-10380.
- Nadagouda MN, Speth TF and Varma R: Microwave-assisted green synthesis of silver nanostructures. *Acc Chem Res.* 2011; 44: 469-478.
- Mahdi S, Taghdiri M, Makari V and Rahimi-Nasrabadi M: Procedure optimization for green synthesis of silver nanoparticles by aqueous extract of *Eucalyptus oleosa*. *Spectrochimica Acta Part A: Molecular and Biomolecular Spectroscopy* 2015; 136: 1249-1254.
- Dada OA, Adekola FA and Odebumi EO: Kinetics and equilibrium models for sorption of Cu(II) onto a novel manganese nano-adsorbent. *Journal of Dispersion Science and Technology* 2016; 37(1): 119-133.
- Rai A, Singh A, Ahmad A and Sastry M: Role of halide ions and temperature on the morphology of biologically synthesized gold nanotri. *Langmuir* 2006; 22: 736-41.
- Prabhu D, Arulvasu C, Babu G, Manikandan R and Srinivasan P: Biologically synthesized green silver nanoparticles from leaf extract of *Vitex negundo* L. induce growth-inhibitory effect on human colon cancer cell line HCT 15. *Process Biochemistry* 2013 (48); 317-324.
- Piao MJ, Kang KA, Lee IK, Kim HS, Kim S and Choi JY: Silver nanoparticles induce oxidative cell damage in human liver cells through inhibition of reduced glutathione and induction of mitochondria-involved apoptosis. *Toxicol Lett* 2011; 201: 92-100.
- Tan P, Hou C, Liu Y, Lin LJ and Cordell GA: Swertipunicoside. The first bisxanthone C-glycoside. *J. Org. Chem.*1991; 56: 7130-7133.

34. Tan P, Liu YL and Hou CY: Structure of swertiapuniside from *S. punicea* Hemsl. National centre for Biotechnology Information (PubMed Journals) 1992; 27: 476-479.
35. Jeyaraj M, Rajesha M, Arunb R, Mubarak Alic D, Sathishkumara G and Sivanandhana G: An investigation on the cytotoxicity and caspase-mediated apoptotic effect of biologically synthesized silver nanoparticles using *Podophyllum hexandrum* on human cervical carcinoma cells. Colloids Surf B: Biointerfaces 2013; 102: 708-17.
36. Saraniya Devi J, Valentin Bhimba B: Anticancer Activity of Silver Nanoparticles Synthesized by the Seaweed *Ulva lactuca*: *In vitro*. Open Access Scientific Reports. 2012 1(4); 1-5.
37. Pandian N and Chidambaram S: Antimicrobial, cytotoxicity and anti cancer activity of silver nanoparticles from *Glycyrrhiza glabra* 2015; 41: 1633.
38. Ramanibai R and Velayutham K: Bioactive compound synthesis of Ag nanoparticles from leaves of *Melia azedarach* and its control for mosquito larvae 2015; 98: 82-88.

How to cite this article:

Sivaranjani S and Arulvasu C: Synthesis of silver nanoparticles using swertipunicoside and its activity on human breast cancer cell line (MCF-7). Int J Pharm Sci & Res 2018; 9(10): 4393-01. doi: 10.13040/IJPSR.0975-8232.9(10).4393-01.

All © 2013 are reserved by International Journal of Pharmaceutical Sciences and Research. This Journal licensed under a Creative Commons Attribution-NonCommercial-ShareAlike 3.0 Unported License.

This article can be downloaded to **ANDROID OS** based mobile. Scan QR Code using Code/Bar Scanner from your mobile. (Scanners are available on Google Playstore)